

THE DISTRIBUTION OF MAXIMUM RELATIVE GRAVITATIONAL TORQUES IN DISK GALAXIES

R. BUTA,¹ E. LAURIKAINEN,² AND H. SALO²
Received 2003 August 4; accepted 2003 September 24

ABSTRACT

The maximum value of the ratio of the tangential force to the mean background radial force is a useful quantitative measure of the strength of nonaxisymmetric perturbations in disk galaxies. Here we consider the distribution of this ratio, called Q_g , for a statistically well-defined sample of 180 spiral galaxies from the Ohio State University Bright Galaxy Survey and the Two Micron All Sky Survey. The ratio Q_g can be interpreted as the maximum gravitational torque per unit mass per unit square of the circular speed and is derived from gravitational potentials inferred from near-infrared images under the assumptions of a constant mass-to-light ratio and an exponential vertical density law. In order to derive the most reliable maximum relative torques, orientation parameters based on blue-light isophotes are used to deproject the galaxies, and the more spherical shapes of bulges are taken into account using two-dimensional decompositions that allow for analytical fits to bulges, disks, and bars. Also, vertical scale heights h_z are derived by scaling the radial scale lengths h_R from the two-dimensional decompositions, allowing for the type dependence of h_R/h_z indicated by optical and near-infrared studies of edge-on spiral galaxies. The impact of dark matter is assessed using a “universal rotation curve” parameterization and is found to be relatively insignificant for our sample. In agreement with a previous study by Block et al., the distribution of maximum relative gravitational torques is asymmetric toward large values and shows a deficiency of low- Q_g galaxies. However, because of the above refinements, our distribution shows more low- Q_g galaxies than that of Block et al. We also find a significant type dependence in maximum relative gravitational torques, in the sense that Q_g is lower on average in early-type spirals than in late-type spirals. The effect persists even when the sample is separated into bar-dominated and spiral-dominated subsamples and also when near-infrared types are used, as opposed to optical types.

Key words: galaxies: kinematics and dynamics — galaxies: spiral — galaxies: structure

1. INTRODUCTION

Nonaxisymmetric features are a pervasive and complex aspect of disk galaxies. In normal, relatively noninteracting galaxies, these features are in the forms of bars or spirals. It is well known that the presence of nonaxisymmetric structures in galaxy disks can impact the evolution of morphology. For example, bars may drive spiral density waves (Kormendy & Norman 1979), generate resonance rings of gas (Schwarz 1981; Buta & Combes 1996), impact abundance gradients (Martin & Roy 1994), or induce gas inflow that may lead to bar destruction and bulge growth (Norman, Sellwood, & Hasan 1996). A spiral may trigger shocks, inducing star formation (Roberts, Roberts, & Shu 1975), or may rearrange stochastically induced star-forming regions into a more organized pattern (McCall 1986). It is clear that nonaxisymmetric features, with their associated pattern speeds and resonances, are extremely important in galactic evolution, and understanding how these features develop is one of the principal problems in galaxy formation and dynamics.

The source of much of the evolution caused by bars and spirals is gravity torques due to tangential forces. Combes & Sanders (1981; see also Sanders & Tubbs 1980) suggested that these forces could provide a useful measure of the strengths of nonaxisymmetric features such as bars if the potential could be determined. The idea is to derive the maximum value of the ratio of the tangential force to the mean

background (or axisymmetric) radial force, which would give a single dimensionless number indicating the relative importance of nonaxisymmetry in the potential of a galaxy. This ratio, which is physically the same as the maximum gravitational torque per unit mass per unit square of the circular speed, will be referred to in this paper as Q_g , while the method for deriving Q_g will be referred to as the gravitational torque method (GTM).

The advent of routine near-infrared imaging of galaxies has made application of the GTM more practical than ever. Near-infrared images trace the stellar mass distribution of galaxies, because of their emphasis on the older, dominant stellar populations. Potentials can be derived from such images using fast Fourier transform techniques in conjunction with assumptions concerning the mass-to-light ratio and the vertical density distribution (e.g., Quillen, Frogel, & González 1994, hereafter QFG). From this potential, the radial and tangential components of the forces in the plane of the galaxy can be derived, and the Combes & Sanders ratio can be estimated. Recent studies by Buta & Block (2001), Block et al. (2001, 2002), Laurikainen, Salo, & Rautiainen (2002), and Laurikainen & Salo (2002) have provided the first attempts to derive the maximum force ratios for significant samples of galaxies. However, in these cases the samples were either ill defined statistically, based entirely on relatively short exposure Two Micron All Sky Survey (2MASS; Skrutskie et al. 1997) near-infrared images, or used deprojected images that did not allow for the typically rounder shapes of bulges or the most reliable estimates of vertical scale heights.

There are good reasons for trying to derive the maximum force ratio for a large, statistically well defined sample of

¹ Department of Physics and Astronomy, University of Alabama, Box 870324, Tuscaloosa, AL 35487.

² Department of Physical Sciences, University of Oulu, Box 3000, FIN-90014 Oulu, Finland.

galaxies using a refined version of the GTM. First, Sellwood (2000) has argued that we could evaluate scenarios of bar formation in disk galaxies if we knew the observed distribution of bar strengths. Various bar formation scenarios, such as the natural “bar instability” (Miller, Prendergast, & Quirk 1970; Hohl 1971; Sellwood & Wilkinson 1993 and references therein) or tidal bar formation (e.g., Noguchi 1996; Miwa & Noguchi 1998) may predict different distributions of maximum relative bar torques, and an observed distribution may distinguish which mechanism is most important. Second, recurrent bar formation due to accretion of external gas would impact the distribution of maximum force ratios (Bournaud & Combes 2002). The idea is that bars can be the engines of their own destruction in the presence of gas (see, for example, Das et al. 2003) but may reform or regenerate later if a galaxy accretes significant quantities of external gas during a Hubble time that may cool the disk sufficiently (see also Sellwood & Moore 1999). Thus, accretion can impact the “duty cycle” of bars. This idea was evaluated by Block et al. (2002) using an application of the GTM to the Ohio State University Bright Galaxy Survey (OSUBGS; Eskridge et al. 2002). Block et al. concluded that the distribution of maximum relative torques favored the idea that galaxies accrete enough gas to double their mass in 10^{10} yr.

In this paper we reexamine the distribution of maximum relative torques in spiral galaxies based on the application of a much refined version of the GTM to basically the same OSUBGS sample as used by Block et al., supplemented by a few larger galaxies with images from the 2MASS database. Our goal is to derive a reliable distribution of maximum relative bar and spiral torques in disk galaxies that can be compared with model predictions. The refinements we use account for the shapes of bulges, improved estimates of the galaxy orientation parameters, vertical scale heights inferred from type-dependent scalings of the radial scale length, and a statistical evaluation of the impact of dark matter. The Q_g values we use are from Laurikainen et al. (2003). Only a few of the technical details connected with these values will be provided here, and we refer the reader to Laurikainen et al. (2003) for a full accounting of our application of the GTM. Our approach allows us to derive the most reliable maximum relative torques and therefore the most accurate distribution of these torques.

2. PROPERTIES OF THE SAMPLE

Our sample consists of 158 galaxies from the OSUBGS having inclinations of less than 65° and 22 2MASS galaxies

having a similar inclination limit but that were too large to be in the OSUBGS. The selection criteria for the OSUBGS are that the Third Reference Catalogue of Bright Galaxies (RC3; de Vaucouleurs et al. 1991) T -index be in the range $0 \leq T \leq 9$ (S0/a to Sm), the total magnitude B_T be ≤ 12.0 , the isophotal diameter D_{25} be $\leq 6'.5$, and the declination be in the range $-80^\circ < \delta < +50^\circ$ (Eskridge et al. 2002). Table 1 summarizes several of the mean properties of the sample, based on data from RC3. Of the 180 galaxies, 177 have family classifications given in RC3. Table 1 shows that in the sample, there are virtually equal numbers of galaxies classified as SA, SAB, or SB. Table 1 divides the averages according to this classification parameter. The table shows that mean parameters in the sample are similar within these families. The mean Hubble type is Sb–Sbc. Average colors, apparent angular size, radial velocities, and distances are similar among the families. There is an indication that, on average, the SA galaxies in the sample are slightly more inclined than the SAB and SB galaxies. Also, SA galaxies are slightly more luminous and larger than SAB and SB galaxies. An inclination effect on the morphological recognition of bars is not unexpected and merely highlights the difficulty of seeing bars that are weak and viewed at high inclination. However, with bulge/disk decomposition and deprojection, as well as near-IR imaging, we can detect some of these lost bars.

Figures 1 and 2 show the more detailed distributions of SA, SAB, and SB galaxies in the sample versus RC3 type, absolute blue magnitude M_B^0 , the logarithm of the isophotal axis ratio $\log R_{25}$, and corrected color index $(B-V)_T^0$. Absolute magnitudes use B_T^0 from RC3 and distances either from or on the scale of Tully (1988). Although the mean T -index is nearly the same for the separate families, SB galaxies are asymmetrically distributed toward early types, while SA galaxies are asymmetrically distributed toward later types. The distributions by absolute magnitude show the higher luminosities of the SA galaxies compared with SAB and SB galaxies. The distribution with $\log R_{25}$ definitely emphasizes lower inclinations for SB galaxies, while it is more uniform for SA galaxies to the cutoff. Integrated colors are similarly distributed over the three families.

For comparison, Figures 3 and 4 show the same histograms for a distance-limited sample of 1264 spirals³ from the catalog

TABLE 1
SAMPLE PROPERTIES^a

Parameter	SA	SAB	SB	SA (T88)	SAB (T88)	SB (T88)
n	58	57	62	291	364	609
$\langle A_B(G) \rangle$	0.15	0.10	0.17	0.19	0.17	0.21
$\langle \log R_{25} \rangle$	0.17	0.15	0.15	0.29	0.21	0.30
$\langle T \rangle$	3.67	3.83	3.61	4.45	5.18	6.46
$\langle \log D_0 \rangle$	1.64	1.66	1.62	1.58	1.51	1.46
$\langle (B-V)_T^0 \rangle$	0.62 (51)	0.61 (49)	0.60 (52)	0.58 (209)	0.56 (219)	0.53 (286)
$\langle (U-B)_T^0 \rangle$	0.06 (41)	0.05 (39)	0.04 (46)	0.00 (169)	-0.03 (175)	-0.07 (256)
$\langle V_\odot \rangle$ (km s ⁻¹).....	1467	1322	1536	1564	1622	1543
$\langle \Delta \rangle$ (Mpc).....	21.0	19.0	20.8	22.3	23.6	21.6
$\langle M_B^0 \rangle$	-20.37	-20.21	-20.22	-19.8	-19.5	-18.7
$\langle D_0 \rangle$ (kpc).....	26.7	25.5	25.4	24.3	22.9	18.5
$\langle Q_g \rangle \pm \sigma$	0.110 \pm 0.065	0.221 \pm 0.122	0.331 \pm 0.147

^a Numbers in parentheses are the sample sizes available for the indicated mean parameters. T88 refers to the catalog of Tully 1988.

³ This number includes only those Tully sample galaxies having RC3 data available.

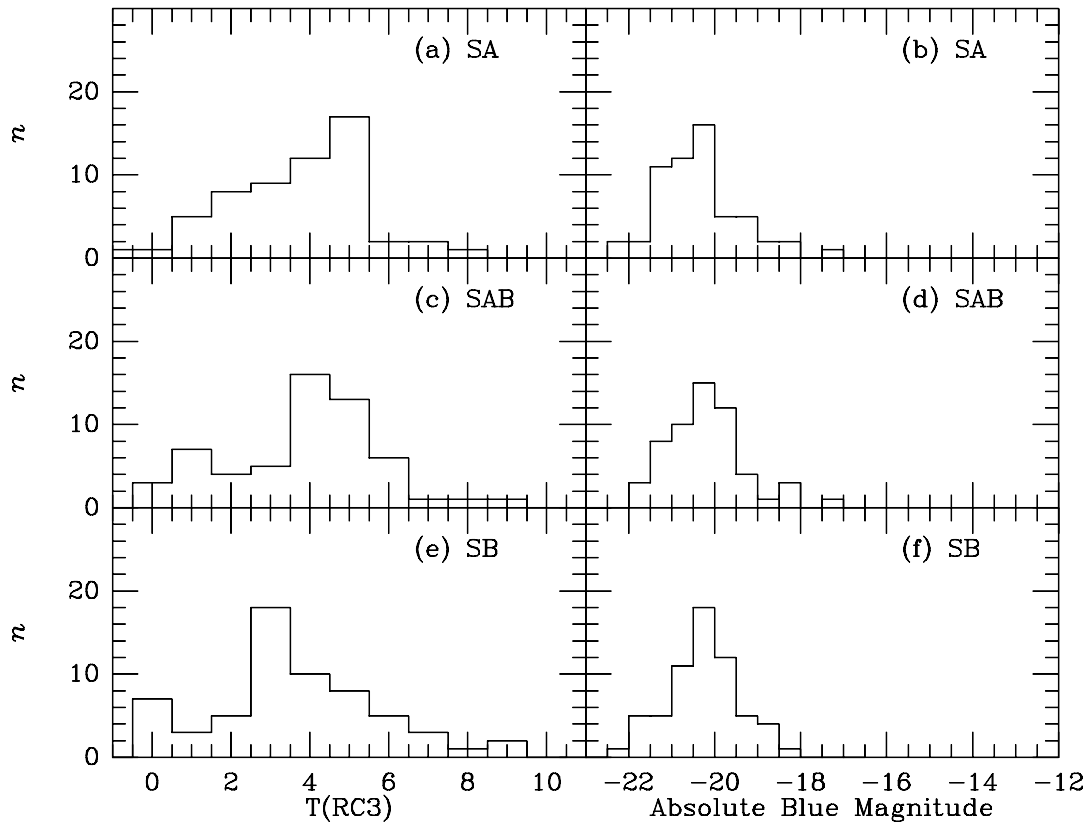


FIG. 1.—Number of sample galaxies, divided into RC3 families, vs. RC3 type index and absolute B -band magnitude, the latter based on RC3 magnitudes B_T^0 and on distances from Tully (1988) or the linear Virgocentric flow model if not in that catalog.

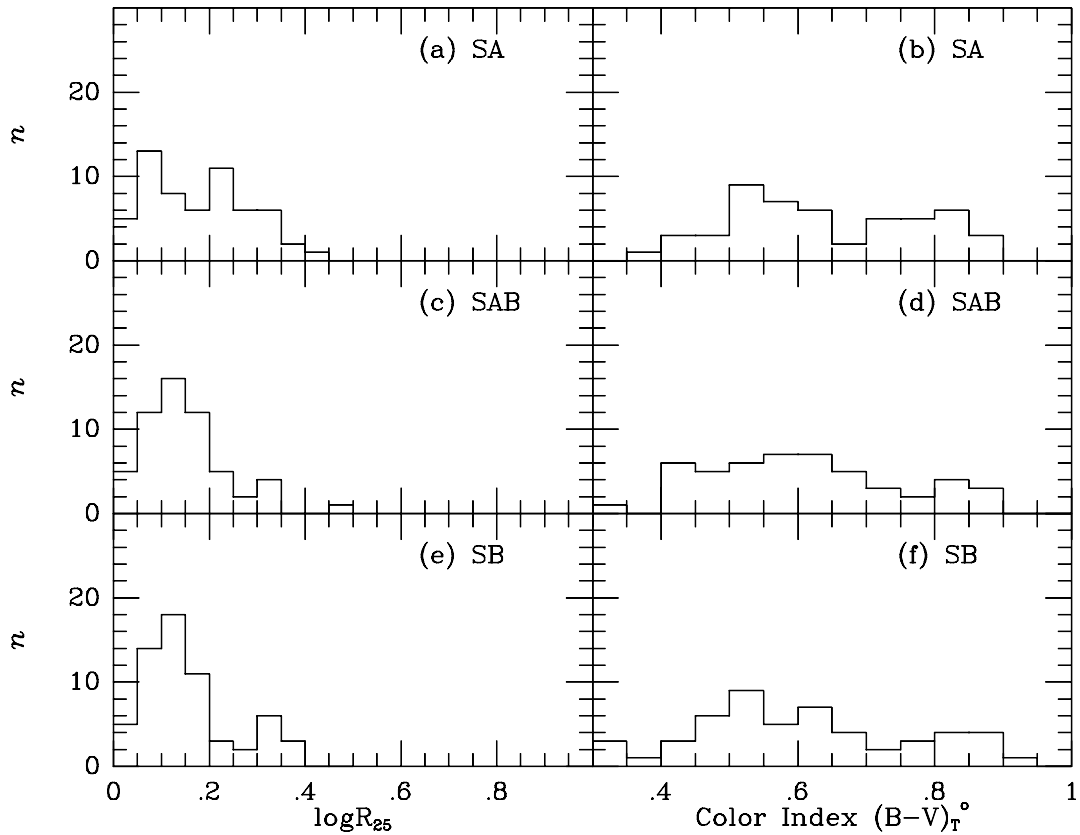


FIG. 2.—Number of sample galaxies, divided into RC3 families, vs. isophotal axis ratio $\log R_{25}$ and total color index $(B-V)_T^0$, both parameters from RC3

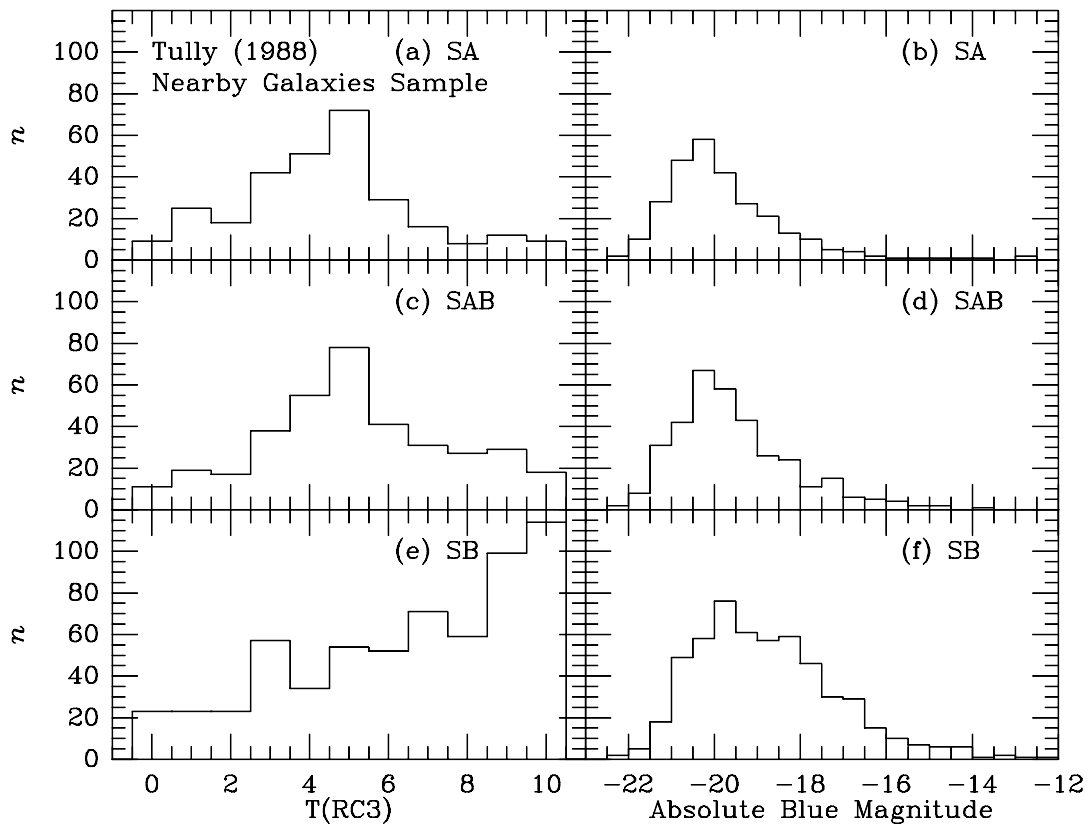


FIG. 3.—Number of galaxies, divided into RC3 families, in the distance-limited sample of Tully (1988) vs. RC3 type index and absolute B -band magnitude, the latter based on RC3 magnitudes B_T^0 .

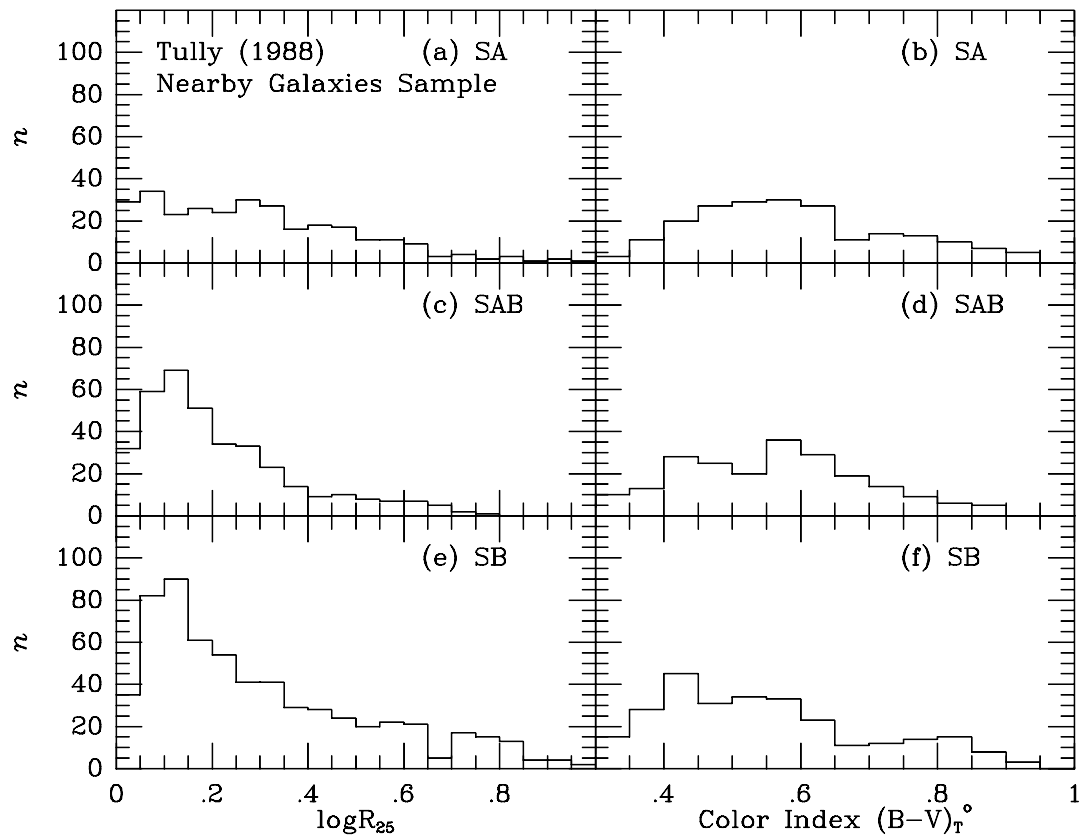


FIG. 4.—Number of galaxies, divided into RC3 families, in the distance-limited sample of Tully (1988) vs. isophotal axis ratio $\log R_{25}$ and total color index $(B-V)_T^0$, both parameters from RC3.

of Tully (1988). Table 1 lists the mean parameters for the same sample. Our magnitude- and diameter-limited OSU/2MASS sample emphasizes earlier Hubble types and brighter absolute magnitudes than the Tully catalog, the differences being most extreme for SB galaxies. The distributions of color and axis ratio, except for our inclination cutoff, are similar to those for our sample galaxies. Thus, our sample is mainly biased against late-type, low-luminosity barred spirals. There is less bias in the SA and SAB subsamples because these tend to have fewer late-type, low-luminosity examples. A critical issue is that it appears that our sample is not necessarily biased much against *nonbarred* spirals.

3. REFINEMENTS TO THE GTM

The basic assumptions in the GTM are that (1) the near-infrared light distribution traces the mass (i.e., the mass-to-light ratio is constant), (2) the vertical density distribution can be simply represented as, for example, exponential with vertical scale height h_z , and (3) galaxies can be deprojected as thin disks, after allowing for the shape of the bulge. As noted by Buta & Block (2001), the first assumption is probably valid for many galaxies in the bar region, where maximum disks tend to be found (e.g., Freeman 1992). However, this is still an open question, as noted by Kranz, Slyz, & Rix (2003), who used the amplitudes of modeled noncircular motions in five spirals to deduce that maximum disks may be valid only if the maximum rotation velocity exceeds 200 km s^{-1} . In our sample, this would be the case only for galaxies having $M_B < -20.8$ (Tully et al. 1988). We address this issue further in § 8 using the “universal rotation curve” approach of Persic, Salucci, & Stel (1996, hereafter PSS). Laurikainen & Salo (2002) showed that the GTM is fairly insensitive to the form of the assumed vertical density distribution.

3.1. Polar versus Cartesian Grid

The first refinement we use over Buta & Block (2001) is a polar coordinate grid as opposed to a Cartesian grid (Laurikainen & Salo 2002). Buta & Block used the QFG method of transforming near-IR images into gravitational potentials, which operates on a two-dimensional image. This approach provides an image of the potential, which can be used to derive a two-dimensional map of the ratio of the tangential to the mean radial force. In such a map, if a strong bar is present, four well-defined maxima or minima are seen in the form of a “butterfly pattern.” Buta & Block defined the bar strength Q_b to be the average of the absolute values of the four maxima/minima.

Laurikainen et al. (2002) and Laurikainen & Salo (2002) used a polar grid approach as an alternative to QFG to allow the application of the GTM to noisy and rather low resolution 2MASS images. Fourier components of the light distribution are computed as a function of radius R and azimuthal angle ϕ , and these Fourier light components are individually transformed into potential components. The potential is then reconstructed analytically, and the maximum force ratio $Q_T = |F_T/F_{0R}|_{\text{max}}$ is computed as a function of radius.

3.2. Orientation Parameters

In previous GTM studies such as those of Buta & Block (2001) and Block et al. (2001, 2002), orientation parameters from RC3 were used to deproject most of the galaxy images. However, these orientation parameters are in many cases

based on photographic images and can be manifestly improved with modern digital images. We have used the B -band images from the OSUBGS to fit ellipses to outer isophotes and derive mean axis ratios and position angles for the outer disks. In the future, these can also be improved upon using two-dimensional velocity fields. The results of the ellipse fits, as well as uncertainties, will be provided by Laurikainen et al. (2003).

3.3. Bulge Shapes

Although the bulges of some barred galaxies might be as flat as the disk (Kormendy 1993), in many galaxies the bulge is a rounder component than the disk. If this rounder shape is ignored when deprojecting a galaxy, the bulge isophotes will be stretched into a barlike distortion (called “deprojection stretch” by Buta & Block 2001), leading to false torques. To deal with this problem we have used two-dimensional photometric decomposition, based on Sérsic models (Sérsic 1968) and allowing for seeing effects. The bulge and disk are described as in Mollenhöff & Heidt (2001), and in addition a bar component is added to the fit (Ferrer’s bar with index $n = 2$), which in some cases is essential for avoiding artificially large bulge models. The technique that we used, as well as the derived parameters, will be outlined in more detail by Salo, Laurikainen, & Buta (2003). The decompositions allowed us to remove the bulges, deproject the disks, and then add back the bulges as spherical components. Thus, our analysis is not affected seriously by bulge deprojection stretch.

3.4. Vertical Scale Height

The computation of a potential from a near-infrared image requires a value for the vertical scale height, which can be directly measured only for edge-on galaxies. Buta & Block (2001) and Block et al. (2001) simply assumed that all galaxies had the same vertical exponential scale height as our Galaxy, $h_z = 325 \text{ pc}$ (Gilmore & Reid 1983). However, this approach required knowledge of the distance to each galaxy, which had to be based on radial velocities. Here we follow Laurikainen et al. (2002) and derive $h_z (=0.5z_0)$, where z_0 equals the isothermal scale height) by scaling values from the radial exponential scale length h_R . As shown by de Grijs (1998), the ratio h_R/h_z depends on Hubble type, being larger for later types compared to earlier types. Values of h_R were provided by our decompositions, and we used the following scalings by type: $h_R/h_z = 4$ for S0/a–Sa galaxies, 5 for Sab–Sbc galaxies, and 9 for Sc galaxies and later.

4. THE MAXIMUM RELATIVE GRAVITATIONAL TORQUE

We define the maximum relative gravitational torque Q_g to be the maximum value of the ratio of the tangential force to the mean radial force derived from a plot of Q_T versus R , based on a quadrant analysis. In some cases, Q_g is mostly measuring the maximum torque due to a bar, while in other cases Q_g is clearly measuring only spiral torques. In many cases, Q_g is measuring a combination of bar and spiral torques, as shown by Buta, Block, & Knapen (2003), who developed a Fourier-based bar/spiral separation technique. Thus, our analysis cannot provide a true distribution of maximum relative bar torques Q_b . For the evaluation of accretion models of spirals, Block et al. (2002) noted that this is not a problem because the models often also have spiral torques that contribute to Q_g estimates.

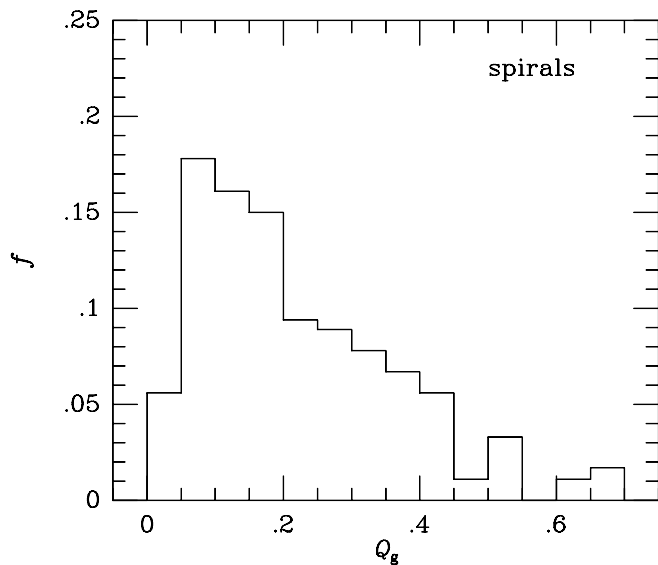


FIG. 5.—Relative frequency of maximum gravitational torques for 180 spiral galaxies.

5. THE DISTRIBUTION OF Q_g VALUES

Our main result is shown in Figure 5 and is compiled as counts n and relative frequencies f ($=n/180$) in Table 2. The distribution of maximum relative gravitational torques is shown for the full sample of 180 galaxies in comparison with the subsamples of SA, SAB, and SB galaxies in Figure 6. The latter plots show again that there is indeed a correlation between maximum torque and de Vaucouleurs family classification, but the spread in Q_g is very wide for SAB and SB galaxies. SA galaxies appear to genuinely select the narrowest range of Q_g values, while SAB and SB galaxies include objects having Q_g values between 0.05 and 0.7. Thus, except for SA galaxies, the de Vaucouleurs family classifications do not tell us much about real gravitational bar torques except in an average sense. In Table 1, the mean values of Q_g by family are listed. The mean increases linearly from SA to SB, with maximum relative gravitational torques being 11% for a typical SA galaxy, 22% for a typical SAB galaxy, and 33% for a typical SB galaxy.

Figure 5 shows an asymmetric distribution of maximum relative gravitational torques, with a “tail” extending to

$Q_g \approx 0.7$. From the histograms in Figure 6, it is clear that the primary peak in this plot is due mainly to SA and SAB galaxies, while the extended tail is due to SAB and SB galaxies. The average value of Q_g for the full sample is 0.222 with a standard deviation of 0.147.

6. DISTRIBUTION UNCERTAINTIES AND A COMPARISON WITH BLOCK ET AL. (2002)

As we have noted, a similar study of the distribution of maximum relative gravitational torques in the OSUBGS sample was made by Block et al. (2002). They selected 163 galaxies from the original sample of 198 having inclinations of 70° or less and not being members of obviously interacting systems. Vertical exponential scale heights were derived from roughly estimated radial scale lengths (see below) as $h_z = h_R/12$. Most importantly, no bulge/disk decompositions were made to allow for the likely rounder shapes of bulges, and approximate orientation parameters from RC3 were used for the deprojections. Like us, however, Block et al. derived Q_g from graphs of Q_T versus R .⁴ Thus, a comparison between our histogram of maximum relative torques and theirs is appropriate.

Figure 7 compares the Block et al. distribution of maximum gravitational torques with our distribution. The Block et al. histogram is not exactly the same as the one published, but is based on a table kindly sent to us by F. Combes. It includes 159 galaxies where the measured Q_g is less than 1. In spite of the similar numbers of objects, the Block et al. sample is missing 13 galaxies that are in our sample and includes 18 galaxies missing from our sample. The differences are in part due to our different inclination cutoffs (65° in our analysis vs. 70° used by Block et al.), as well as the different axis ratios used to estimate inclinations (isophotal fits for our sample vs. RC3 $\log R_{25}$ for Block et al.). To make the comparison fair, we use only the 145 galaxies in common between our samples. Although both histograms are similar in showing an asymmetric distribution, our distribution shows more galaxies having low maximum relative torques ($Q_g \leq 0.15$). The first two bins in the Block et al. histogram are extremely deficient in galaxies, a point

⁴ Block et al. (2002) use the term Q_b for their parameter, but it is not derived in the same manner as the Q_b defined by Buta & Block (2001). Instead, it is the same as our definition of Q_g .

TABLE 2
DISTRIBUTION OF MAXIMUM RELATIVE TORQUES

Q_g	n	f
0.025.....	10	0.056
0.075.....	32	0.178
0.125.....	29	0.161
0.175.....	27	0.150
0.225.....	17	0.094
0.275.....	16	0.089
0.325.....	14	0.078
0.375.....	12	0.067
0.425.....	10	0.056
0.475.....	2	0.011
0.525.....	6	0.033
0.575.....	0	0.000
0.625.....	2	0.011
0.675.....	3	0.017

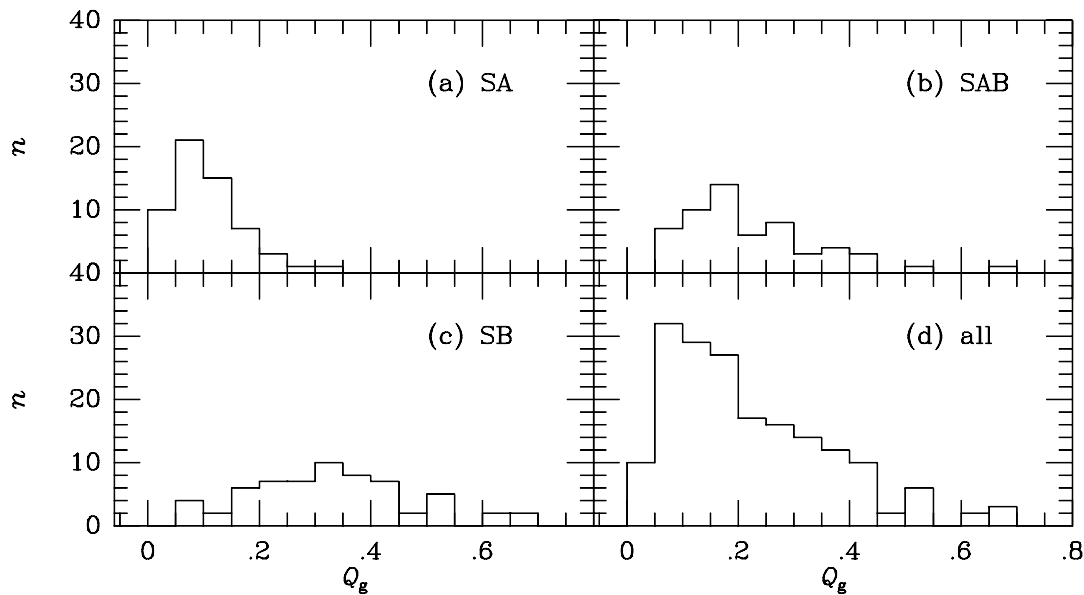


FIG. 6.—Number of galaxies, divided into RC3 families and for the full sample, vs. the maximum relative gravitational torque Q_g for the OSUBGS/2MASS sample of 180 galaxies.

used by them to argue that galaxies double their mass by accretion in 10^{10} yr. The reasons for the differences can be tied directly to a number of causes, highlighted by the histograms in Figure 8. Figure 8a shows that without the correction for bulge shape, deprojection stretch can depopulate the first two bins. However, the effect seems less important than might have been expected given that our inclination cutoffs were high in both cases. A more serious effect could be the assumed scale heights, as shown in Figure 8b. In this plot we allow for the scatter in h_R/h_z from de Grijs (1998) and compute Q_g for the minimum values of $h_R/h_z = 1, 3,$ and 5 (“max h_z ” case) and maximum values of $5, 7,$ and 12 (“min h_z ” case) for types S0/a–Sa, Sab–Sbc, and Sc and later, respectively. The “max h_z ” case clearly shows

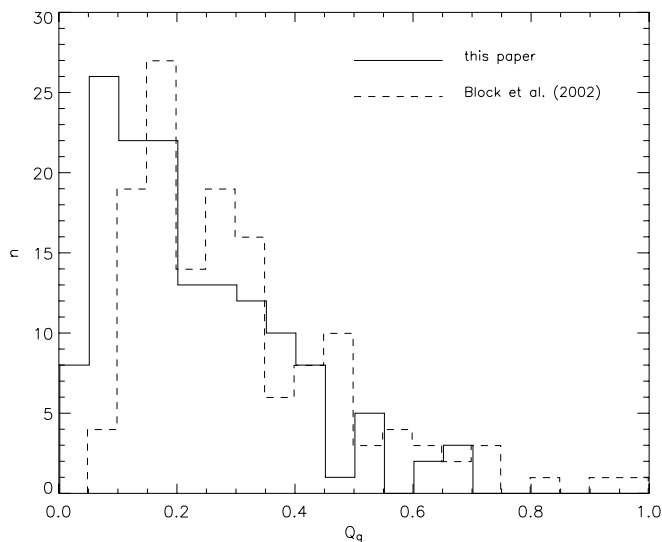


FIG. 7.—Comparison of the distribution of maximum relative gravitational torques Q_g for this paper (solid histogram) and Block et al. (2002) (dashed histogram). The comparison sample includes 145 galaxies from the OSUBGS only (see text).

more low Q_g values than the “min h_z ” case. Since Block et al. (2002) used $h_R/h_z = 12$ for all galaxies irrespective of Hubble type, their analysis favored lower vertical scale heights and larger values of Q_g on average. Our use of bulge/disk decompositions and a type dependence to h_R/h_z means that on average, our vertical scale heights are higher than those used by Block et al. (2002), and hence our gravitational torques are weaker. For a fairer comparison, we have recomputed Q_g for our deprojected images assuming $h_z = h_R/12$. As expected, this depletes the first two bins but does not account for all the differences seen. The use of improved orientation parameters could also contribute a little to the differences.

Figures 8c and 8d show that uncertainties of $\pm 5^\circ$ in inclination and $\pm 4^\circ$ in major-axis position angle do not impact the observed distribution of gravitational torques too seriously. The number of Fourier terms to $m = 20$ (Fig. 8f) also has little impact.

Figure 8e shows the histograms for those galaxies where Q_g is clearly measuring a bar mostly and those where Q_g is clearly measuring a spiral. The distinction was made by examining the phase of the $m = 2$ component in the region of the maximum. If this phase was relatively constant, then we concluded that the Q_T plot was bar-dominated at the radius of the Q_g maximum. Otherwise, we concluded that it was spiral-dominated. Both distributions show a wide spread, although spirals are weaker on average than bars.

Table 3 summarizes the uncertainties in individual estimates of Q_g due to inclination, position angle, and vertical scale height. Here inclination i is computed using either our mean ellipse-fit axis ratios for the OSUBGS sample or $\log R_{25}$ for the 2MASS sample. We assume the galaxies are oblate spheroids with an intrinsic axis ratio of $q_0 = 0.2$. The table compiles the average deviation for $i \pm 5^\circ$, $\phi \pm 4^\circ$, and the minimum and maximum values of h_z for three bins of inclination.

In Table 4 and Figure 9, we look for any systematic effects due to inclination. Figure 9 shows plots of Q_g versus inclination i for the three de Vancouleurs families as well as

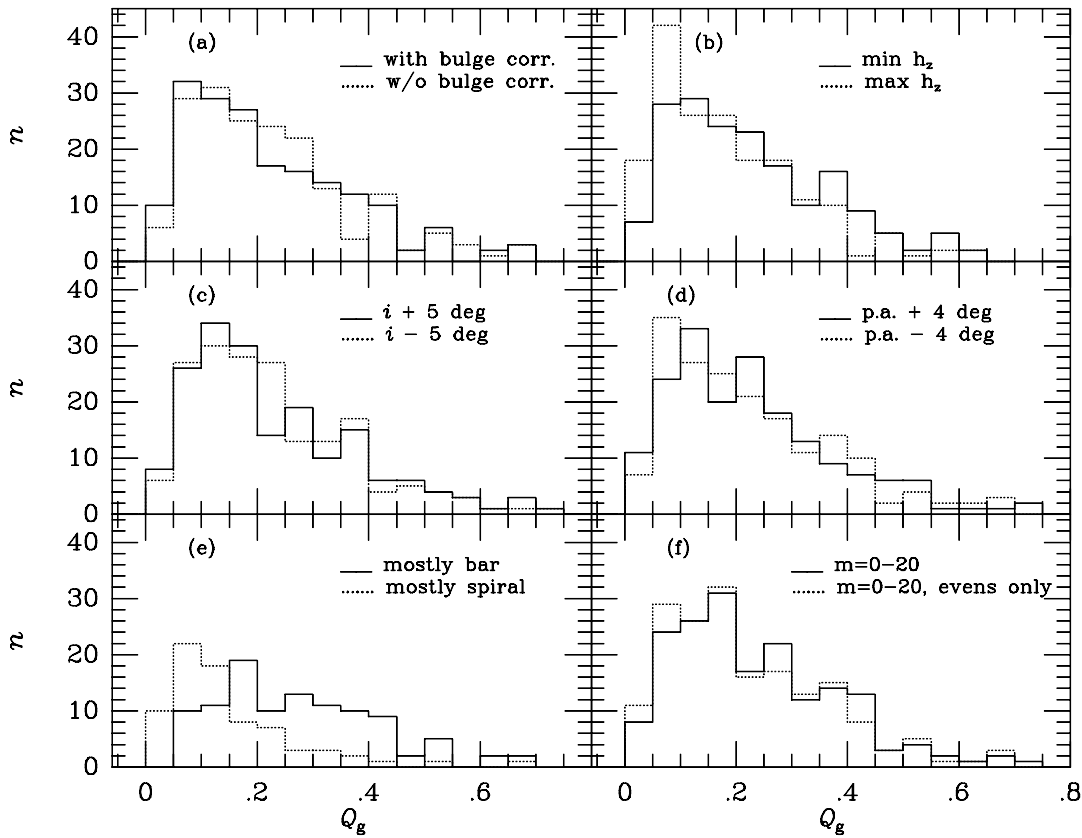


FIG. 8.—Histograms highlighting the impact of uncertainties due to (a) bulge correction, (b) vertical scale height, (c) inclination, (d) major-axis position angle, (e) bar and spiral diagnostics, and (f) number of Fourier terms on the distribution of maximum relative gravitational torques.

the full sample. The figure shows no strong systematic effect with inclination. This is verified in Table 4, where we compile the mean Q_g values for each sample in Figure 9 divided around the median: 45.6° for the SA sample, 40.7° for the SAB sample, 42.6° for the SB sample, and 42.7° for the full sample. Except for the SAB sample, the high- and low-inclination samples have the same means within the mean errors.

Another issue related to uncertainties is the impact of the position angle of the bar relative to the line of nodes. Buta & Block (2001) showed that in a case such as NGC 1300, where the bar is oriented nearly along the line of nodes, the maximum torque is very sensitive to the assumed inclination. The same would be true if the bar were viewed end-on. We have investigated how important this might be in our current sample. Figure 10 shows a plot of Q_g versus relative bar position angle ϕ_b . In this plot, ϕ_b is determined from the phase of the $m = 2$ component of the potential at the radial location where Q_T attains a maximum; the direction in the disk plane is then projected onto the sky plane. Analysis of Figure 10 indicates that there is indeed a bias in the sense

that the average bar strength is weaker for those systems where the bar becomes “thicker” in deprojection. The averages are

$$\langle Q_g \rangle = \begin{cases} 0.223 & \phi_b < 30^\circ, \\ 0.303 & \phi_b > 30^\circ. \end{cases}$$

The solid line in the plot shows the running mean of Q_g in 15° wide bins. The difference is statistically significant, with the probability of having the same true mean values being only 0.0035.

The referee has questioned whether our use of a polar grid approach might cause lower values of Q_g to be measured. The idea is that smoothing with a polar grid might reduce the strength of the perturbation, increasing the number of low Q_g values. We have checked this by recomputing our Q_g values using a Cartesian approach with a 128×128 grid resolution (covering the whole galaxies usually, but not necessarily the whole image). The radial profiles $Q_T(R)$ were constructed

TABLE 3
UNCERTAINTIES

(i)	$\langle Q_g \rangle$	Average Deviation for $i \pm 5^\circ$	Average Deviation for P.A. $\pm 4^\circ$	Average Deviation for h_z	n
24.0.....	0.237	0.010	0.009	0.032	39
40.5.....	0.237	0.019	0.010	0.027	83
58.5.....	0.190	0.038	0.020	0.021	58

TABLE 4
INCLINATION EFFECTS

SAMPLE	n	$\langle Q_g \rangle \pm \text{MEAN ERROR}$			
		$i \leq i_{\text{median}}$	σ	$i \geq i_{\text{median}}$	σ
SA	58	0.115 ± 0.015	0.080	0.104 ± 0.009	0.046
SAB.....	57	0.245 ± 0.026	0.141	0.196 ± 0.018	0.094
SB.....	62	0.325 ± 0.027	0.148	0.336 ± 0.027	0.148
Full.....	180	0.233 ± 0.016	0.151	0.211 ± 0.015	0.143

separately for four image quadrants, and the mean of these profiles was computed. The Cartesian Q_g was then taken from the peak of the Cartesian $Q_T(R)$ profile, limited to the radial range around the force maximum found by the polar method. This was done to insure that the Cartesian Q_g corresponds to the bar region and does not refer to some spurious force maximum in the outer parts of the images. Figure 11 (*top*) shows the results of the comparison. We find very good agreement between our Q_g estimates from the Cartesian and polar grid approaches. However, comparison of the same numbers with the Block et al. (2002) values is poorer, as shown by the top middle and top right panels of Figure 11.

The top left panel of Figure 11 does show that some Cartesian Q_g values are noticeably larger than the polar grid values. However, as discussed in Laurikainen & Salo (2002), the Cartesian method can lead to large spurious force values in the noisy outer parts of images, sometimes leading to an overestimate of Q_g if the results are automatically collected, without careful inspection of the force profiles. This might account for several very large values of Q_b estimated by Block et al. (2002), seen in the top panels of Figure 11. Mainly for this reason, we chose the polar grid force evaluation as our standard procedure. The Cartesian method is useful as a check of the polar method results.

As a further check on how our methods affect the histogram of maximum relative torques, we have analyzed more closely three highly inclined galaxies in our sample, NGC 3166, 3338, and 3675, trying to duplicate the methods used by Block et al.: (1) using the RC3 position angle and inclination to deproject

the galaxies, (2) making no correction for the shape of the bulge, (3) deriving the radial scale length from $\log D_{25}$ in RC3 assuming that all the galaxies follow the Freeman (1970) law, with $h_z = h_R/12$, and (4) using a Cartesian transformation for the potential. The results are $Q_g = 0.26, 0.16,$ and 0.15 , respectively, compared with the values of $0.27, 0.14,$ and 0.15 actually derived by Block et al. Thus, mimicking the Block et al. treatment with our codes yields values that fully agree with those obtained by Block et al. In contrast, our refined approach gives values of $Q_g = 0.11, 0.08,$ and 0.08 for the same galaxies. The reason for the low Q_g values that we get compared with theirs is due to our refinements, not a serious difference in our codes.

The idea that galaxies might accrete significant quantities of external gas during a Hubble time is certainly intriguing. Our revised histogram (with its extended tail of large Q_g values) still supports this idea but may favor an accretion rate between the two cases discussed by Block et al. (2002): the no-accretion idea and a rate that doubles the mass in 10^{10} yr. As shown in this work, the bulge correction, improvements in the orientation parameters, and larger vertical scale heights used considerably increase the number of galaxies with low maximum relative torques.

In spite of the differences with Block et al., we still find a deficiency of galaxies in the lowest torque bin, $Q_g \leq 0.05$. Truly axisymmetric galaxies appear to be rare in the OSUBGS and 2MASS samples, although we note that because Q_g cannot be negative, noise could also deplete the first bin to some extent.

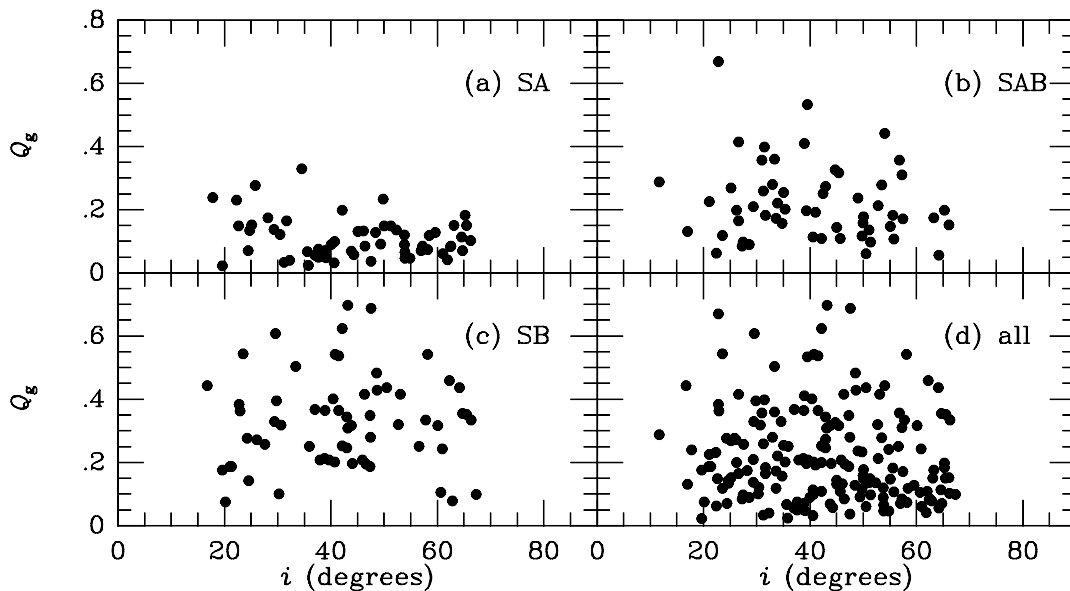


FIG. 9.—Plots of Q_g vs. inclination i for the SA, SAB, SB, and full samples

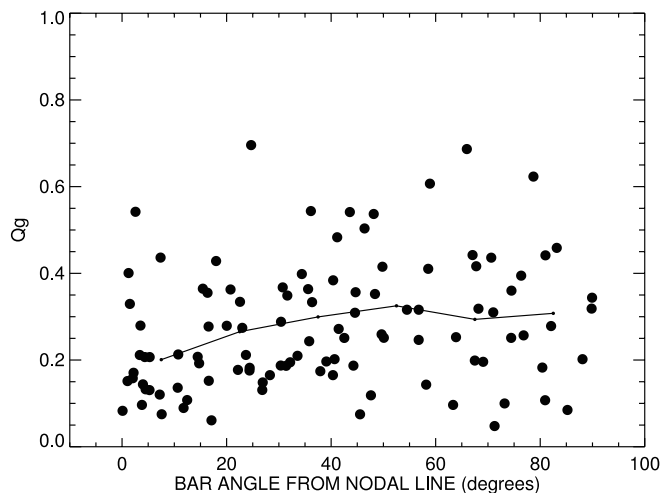


FIG. 10.—Plot of Q_g vs. relative projected bar position angle ϕ_b . The solid curve is the running mean of Q_g in 15° bins.

7. COMPARISON WITH THE f_{bar} PARAMETER

Whyte et al. (2002) have used the OSUBGS to compute bar strength using an isophotal analysis. They derived a bar strength parameter f_{bar} based on the minimum H -band isophotal axis ratio $(b/a)_{\text{bar}}$ in the bar region estimated from a moment analysis involving a series of cuts through an image in surface brightness (Abraham & Merrifield 2000). The parameter f_{bar} is convenient because it scales the bar strength to the range 0.0–1.0 and also because it stretches the range corresponding to the important small $(b/a)_{\text{bar}}$ values. Block et al. (2002) used the Whyte et al. results to support their findings of few nonbarred galaxies in the OSU database and thus their conclusions concerning the accretion rate in galaxies.

The bottom panels of Figure 11 show comparisons between our Q_g values (both polar and Cartesian) and f_{bar} and Q_b (Block et al.) and f_{bar} . The most striking difference is how well f_{bar} correlates with our values of Q_g , showing that the shape of the bar does correspond well to the strength of the gravity field. This was also shown by Laurikainen et al. (2002) for their 2MASS sample. In contrast, the comparison between f_{bar} and Q_b (Block et al.) shows a noticeably larger scatter.

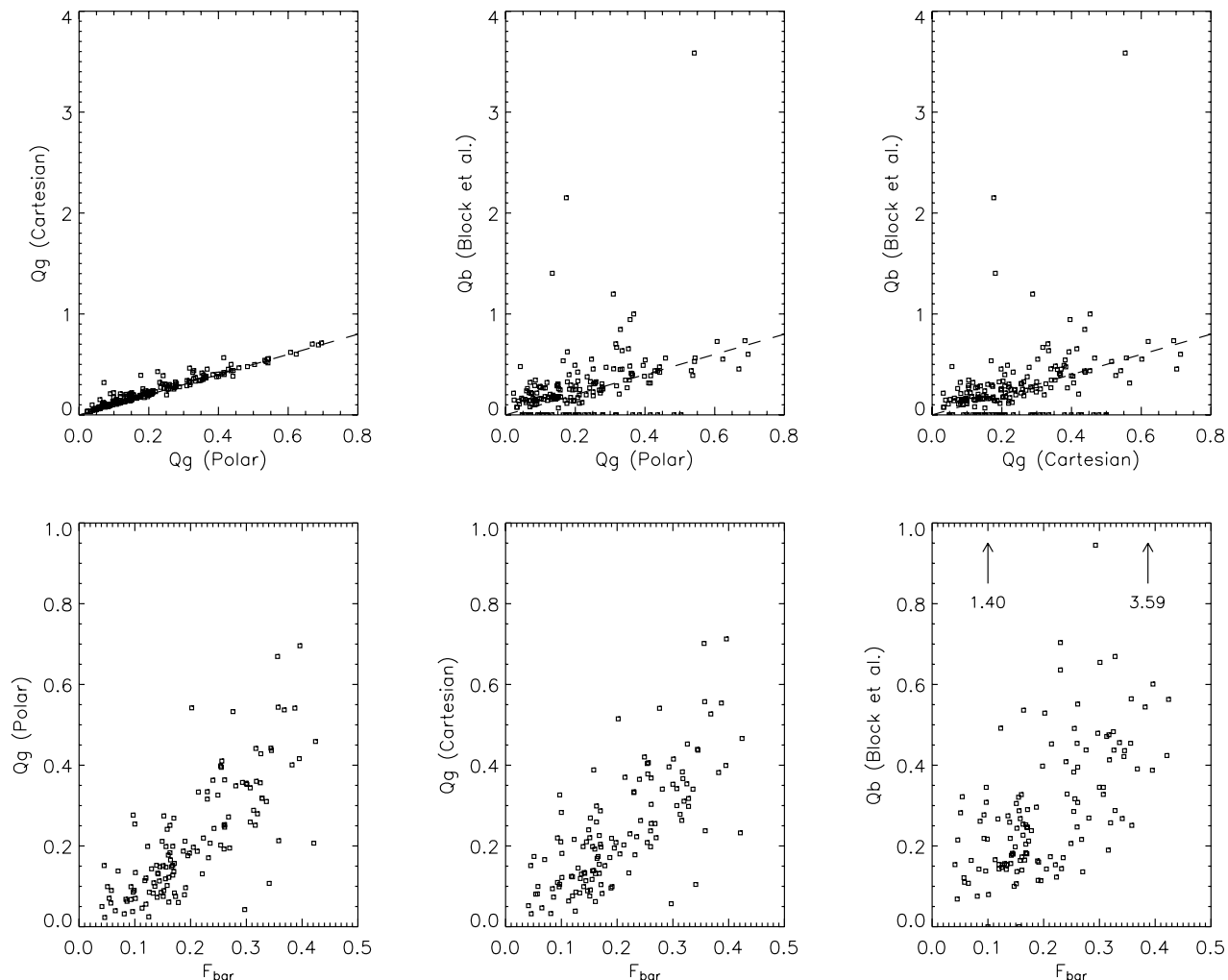


FIG. 11.—*Top*: Comparisons of Q_g estimated using Cartesian and polar grid approaches to estimating the gravitational potential. The top left panel compares our estimates from both approaches, while the top middle and top right panels compare our values with the Q_b estimates of Block et al. (2002). *Bottom*: Plots of our estimates of Q_g from polar and Cartesian grid approaches and the Q_b estimates of Block et al. (2002) vs. the Whyte et al. (2002) bar strength parameter f_{bar} .

In spite of the good agreement between f_{bar} and our Q_g values, f_{bar} is by no means a suitable replacement for Q_g ; f_{bar} is probably determined by the self-consistent response of the bar to the gravitational field that maintains it, and thus it measures the force in an indirect fashion. On the other hand, Q_g estimates this field directly from the luminosity distribution.

8. THE IMPACT OF DARK MATTER

Ideally, the way to assess the impact of dark matter on a torque indicator such as Q_g would be to compare an observed rotation curve with a rotation curve predicted from an azimuthally averaged light profile, preferentially a near-infrared profile corrected for color effects due to a radial stellar population change (e.g., Bell & de Jong 2001). Then the signature of the dark component would be how much the observed and predicted rotation curves disagree, especially in the outer parts of the galaxies. However, it is impractical for us to carry out such a comparison for our full sample in a homogeneous way. Thus, we have used a more statistical approach.

Our estimates for halo corrections are based on the extensive analysis of rotation curves and light profiles by PSS. In this paper the dark halo rotation curves are described by the isothermal sphere law, with a smooth transition to constant core density

$$V_h^2(x) = V_\infty^2 \frac{x^2}{x^2 + a^2}, \quad (1)$$

where $x = R/R_{\text{opt}}$ is the radius normalized to the optical radius, a fiducial reference radius enclosing 83% of the total blue luminosity.⁵ The parameter a is the halo core radius, also in units of R_{opt} . PSS (see especially their erratum) give, based on their sample of 1100 optical and radio rotation curves,

$$a = 1.5 \left(\frac{L}{L_*} \right)^{0.2}, \quad (2)$$

$$\frac{\text{dark mass}}{\text{visible mass}} = 0.4 \left(\frac{L}{L_*} \right)^{-0.9} (x^3) \frac{1 + 1.5^2 (L/L_*)^{0.4}}{x^2 + 1.5^2 (L/L_*)^{0.4}}, \quad (3)$$

where $L_* = 10^{10.4} L_\odot$ in the B band. Near the optical radius we can estimate

$$\frac{\text{dark mass}}{\text{visible mass}} \approx \frac{V_h^2}{V_d^2}, \quad (4)$$

where V_d includes the rotation velocity due to the disk plus bulge.

Equations (1)–(3) now define V_h at all radii, as a function of L/L_* , and the value of $V_d(x)$ at some value near $R = R_{\text{opt}}$. Once $V_h(R)$ is known, the $Q_T(R)$ profiles computed under a constant M/L assumption are modified to

$$Q_T^{\text{hc}}(R) = \frac{Q_T(R)F_d(R)}{F_d(R) + F_h(R)}, \quad (5)$$

where $F_d(R) = V_d(R)^2/R$ and $F_h(R) = V_h(R)^2/R$ are the radial forces due to visible and dark masses, respectively, and the superscript “hc” means “halo-corrected.” If the measurements extend to $R = R_{\text{opt}}$, then $V_d(x=1)$ has been used, while in the case $R_{\text{max}} < R_{\text{opt}}$, $V_d(x = R_{\text{max}}/R_{\text{opt}})$ was used for fitting V_h . Values of R_{opt} were taken from RC3, and the B -band luminosities L were calculated from B magnitudes and Galactic extinctions given in NED and distances from Tully (1988).

Figure 12a shows the distribution of L/L_* for our sample of 180 galaxies. The distribution peaks near $L/L_* \approx 1$. Figure 12b shows the distribution of Q_g^{hc}/Q_g as a function of L/L_* , indicating how the correction becomes more important for less luminous galaxies with more dominant halo components. The deviating point at $L/L_* \approx 1.3$ is NGC 7213, for which Q_g is practically zero and obtained near R_{opt} (Q_g changes from 0.023 to 0.017). Finally, Figure 12c shows the distribution of Q_g with and without halo correction. The average value of Q_g with the correction is 0.209 compared with 0.222 without the correction, indicating only a marginal (6%) reduction.

Altogether, the effect of dark halos appears to be weak for the sample, which as we have shown is dominated by fairly luminous systems for which PSS models imply halos with rather large core radii and relatively small mass within R_{opt} . Therefore, the contribution to $Q_T(R)$ is small in the inner parts of the galaxy where maximum Q_g values are typically obtained, at least for bars. For spiral forces alone the effect would be more prominent.

A potential problem with the fits described above for low-luminosity galaxies is that in many cases the measurements probably do not reach far enough, in terms of disk scale lengths, to yield reliable outer rotation curves (truncation of the disk overestimates the disk radial force and thus the rotation velocities). For Q_g measurements this is not a problem, as noted by Laurikainen & Salo (2002). However, the above procedure uses outer V_d values to estimate V_h values, which therefore might in some cases be overestimated. Indeed, strange, strongly rising rotation curves follow for some of the less luminous galaxies when the above procedure is applied (although they are rising already before inclusion of the halo). Nevertheless, since this error in all cases overestimates the reduction of Q_g due to the inclusion of a halo, it is not important for the present purpose.

9. TYPE DEPENDENCE OF MAXIMUM RELATIVE GRAVITATIONAL TORQUES

Because the bulge is usually more significant in early-type galaxies, we might expect that maximum relative gravitational torques would be diluted somewhat compared to later type galaxies. This is because the bulge can be a significant contributor to the mean axisymmetric radial force in the bar regions of early-type spirals. Block et al. (2001) searched for this effect in their combined sample of 75 galaxies but did not detect a measurable type dependence. They argued that the bulge dilution at early types could be partly offset by the shorter bars found at later types (e.g., Elmegreen & Elmegreen 1985).

Laurikainen et al. (2002) also searched for a type dependence in Q_g in a 2MASS sample of 43 barred galaxies, half of which have active galactic nuclei. In their sample, 19 galaxies have types Sa–Sb and 21 galaxies have types Sbc and later. These authors derived $\langle Q_g \rangle = 0.25 \pm 0.03$ for the early types

⁵ For this radius we have actually used $D_{25}/2$, which is specifically valid only for a Freeman disk. The error committed for those galaxies that may not be Freeman disks is not serious given the approximate nature of these estimates.

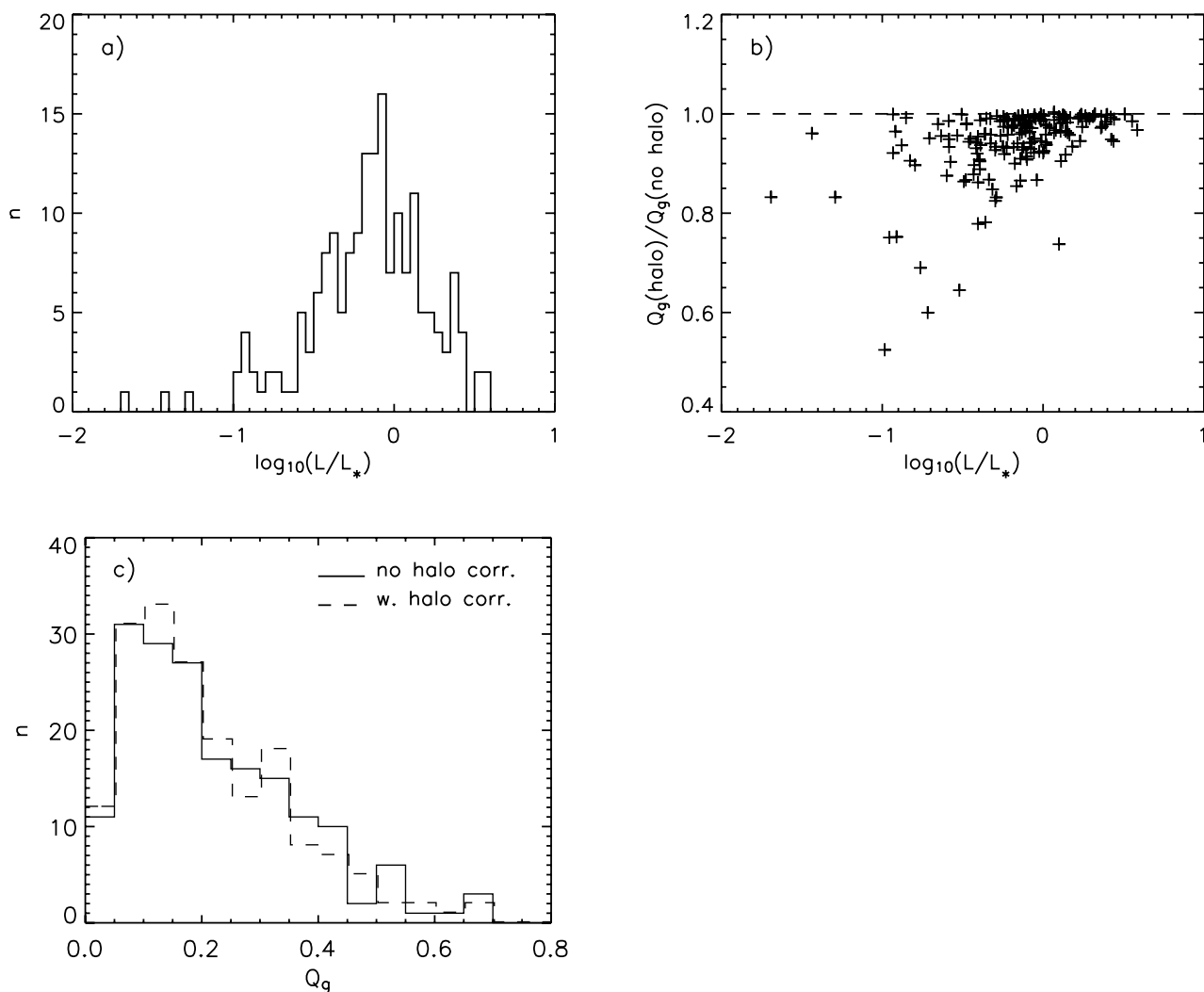


FIG. 12.—(a) Distribution of L/L_* for the sample galaxies, peaking near $L/L_* = 1$. (b) Distribution of Q_g^{hc}/Q_g (with/without halo correction), as a function of L/L_* , indicating how the correction becomes more important for less luminous galaxies with more dominant halo components. The deviating point at $L/L_* \approx 1.3$ is NGC 7213 (see text). (c) Distribution of Q_g with and without halo correction. The similarity of the histograms shows that dark matter has only a small impact on our results.

and 0.38 ± 0.05 for the later types, suggesting a possible difference.

Our refined treatment of bulges and our larger sample compared to these previous studies allows us to reevaluate this possible effect more reliably. As we have noted, we allowed for the more spherical shapes of bulges using two-dimensional photometric decompositions that took into account, where necessary, the contributions of bars. We also treated bulges as spherical in their potentials, such that the forces in the plane are properly estimated. In Buta & Block (2001) and Block et al. (2001), bulges were assumed to be as flat as disks, which overestimated their radial forces in the plane.

Figure 13 shows the correlation of $\langle Q_g \rangle$ with RC3 revised Hubble type in our present sample. The filled circles show the averages with no dark halo correction, while the crosses show the averages with a halo correction. Table 5 also summarizes the numerical values for no halo correction. This plot does appear to detect a type dependence in our measured maximum relative gravitational torques. For early-type spirals ($T = 0-3$, or S0/a–Sb), $\langle Q_g \rangle = 0.177 \pm 0.014$, while for late-type spirals

($T = 4-9$, or Sbc–Sm), $\langle Q_g \rangle = 0.258 \pm 0.015$. A halo correction reduces these means only slightly, to 0.169 for S0/a–Sb and 0.247 for Sbc–Sm. The difference between early- and late-type spirals appears to be significant. As shown in Figure 13 and Table 4, the effect persists even when the sample is divided into de Vaucouleurs families, and it has the same trend in the sense that early types have lower average Q_g values. This suggests that early-type spirals do indeed have diluted maximum relative gravitational torques, an effect that must contribute to the observed scatter of Q_g among the three de Vaucouleurs families.

In interpreting this result, the first question one might ask is how reliable the bulge decompositions are. Since we used a sophisticated two-dimensional decomposition allowing for a bulge, a disk, and a bar in the fit, we believe the decompositions are as good as we can make them. The referee argues that bulge subtraction is delicate and not unique and that if the bulge participates in the bar instability (as in the box/peanut shape), then its impact may not be reliably treated. This is a valid concern. However, Laurikainen & Salo (2002) have tested a radius-dependent scale height that simulates a peanut-shaped

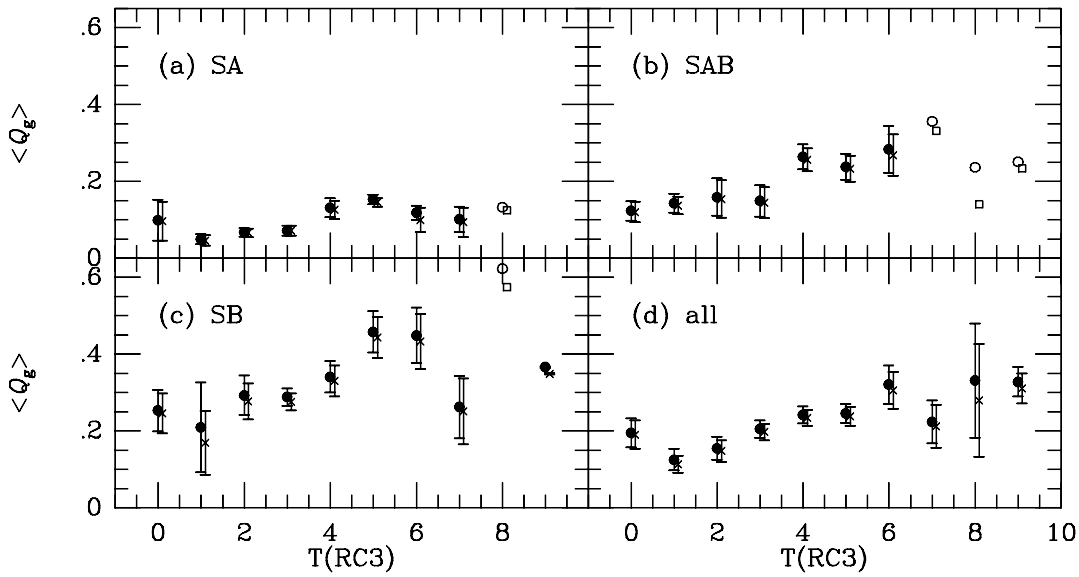


FIG. 13.—Mean maximum relative torque vs. RC3 type index. Error bars are mean errors. The filled circles show the means for no dark halo correction, while the open circles indicate points based on only one galaxy. The crosses show the means with a dark halo correction and are offset by 0.1 in T for clarity. Open squares indicate halo-corrected values based on only one galaxy.

distribution in the sense that the vertical scale height increases toward the outer parts of the bar by an amount similar to that observed in real galaxies. This was found to affect Q_g estimates by only about 5%.

Another important question is how our assumptions concerning the vertical scale height contribute to the observed type dependence. Our estimates of Q_g have utilized the findings of de Grijs (1998) to infer h_z from h_R , assigning larger values of h_z to early types compared to late types. If we assume instead that $h_z = h_R/12$ for all types, we get the results shown in Figure 14. Our assumption of a type dependence to h_R/h_z does indeed enhance the measured type dependence in Q_g . However, the assumption of a constant value of h_R/h_z is inconsistent with studies of edge-on galaxies and favors our approach.

Figure 13 shows that $\langle Q_g \rangle$ is type-dependent, but it does not prove unequivocally that this means bars are relatively weaker

in early-type spirals than in late-type spirals. This is because Q_g is also affected by spiral arm torques. To try to approximately separate the two phenomena, we use the bar/spiral discriminations from Figure 8e and discussed in § 6. If we compute $\langle Q_g \rangle$ as a function of type for these subsamples separately, we get the results in Figure 15. Surprisingly, it appears that both bars and spirals are relatively weaker in early types as compared to late types. For bars especially, the type dependence is remarkably well defined.

A type dependence in bar strength is also found in the Whyte et al. (2002) analysis, although it is smaller than that found for Q_g . Figure 16 shows $\langle f_{\text{bar}} \rangle$ versus RC3 type index T . Just as for Q_g , early-type spirals have lower average f_{bar} than late types. For 49 S0/a–Sb galaxies in the Whyte et al. sample, $\langle f_{\text{bar}} \rangle = 0.190 \pm 0.013$, while for 76 Sbc and later galaxies, $\langle f_{\text{bar}} \rangle = 0.213 \pm 0.011$. The effect is marginal but is still in the same sense as found for Q_g .

TABLE 5
MEAN MAXIMUM RELATIVE TORQUE BY OPTICAL REVISED HUBBLE TYPE

Stage	$T(\text{RC3})$	$\langle Q_g \rangle$	σ	Mean Error	n
S0/a	0	0.195	0.131	0.038	12
Sa.....	1	0.125	0.108	0.028	15
Sab.....	2	0.155	0.124	0.030	17
Sb.....	3	0.205	0.129	0.023	32
Sbc.....	4	0.242	0.140	0.022	39
Sc.....	5	0.246	0.155	0.025	38
Scd.....	6	0.321	0.180	0.050	13
Sd.....	7	0.224	0.137	0.056	6
Sdm.....	8	0.331	0.258	0.149	3
Sm.....	9	0.328	0.066	0.038	3
S0/a–Sb.....	0–3	0.177	0.126	0.014	76
Sbc–Sm.....	4–9	0.258	0.153	0.015	102
SA0/a–SAb.....	0–3	0.068	0.038	0.008	24
SAbc–SAm.....	4–9	0.139	0.064	0.011	34
SAB0/a–SABb.....	0–3	0.145	0.073	0.017	19
SABbc–SABm.....	4–9	0.260	0.124	0.020	38
SB0/a–SBb.....	0–3	0.274	0.118	0.021	33
SBbc–SBm.....	4–9	0.395	0.152	0.028	29

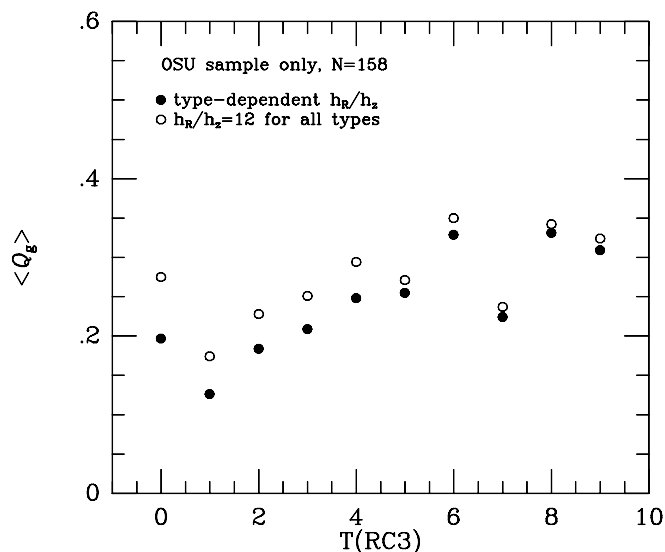


FIG. 14.—Mean maximum relative torque vs. RC3 type index for our full sample using the type-dependent ratio h_R/h_z from de Grijs (1998) and a type-independent ratio $h_R/h_z = 12$ used by Block et al. (2002). Only OSUBGS galaxies are in these samples.

On the basis of theoretical models, one might expect early-type galaxy bars to have stronger maximum torques simply because the bars are longer than those in later types (Elmegreen & Elmegreen 1985). Apparently, bulge dilution is a more dominant effect, so that late-type galaxy bars are stronger in a relative sense. Note that this result refers mainly to Sbc–Sc galaxies as late types, since our sample has few galaxies of types Scd and later. This is a result of our sample biases. A distance-limited sample would provide more reliable results for the very late type spirals.

10. CORRELATIONS WITH NEAR-INFRARED MORPHOLOGY

Eskridge et al. (2002) used the H -band images in the OSUBGS to estimate near-IR classifications of galaxies within the revised Hubble framework of de Vaucouleurs (1959) and Sandage & Bedke (1994). These classifications include the family (SAB or SB and plain S for nonbarred galaxies) and the stage from S0 to Sm. We converted the H -band stages, estimated as if the images were blue-light images, to the RC3 numerical T -index scale. Eskridge et al. (2002) note that the apparently increased bulge-to-disk ratio and the greater degree of smoothness of structure biases near-IR classifications toward earlier types on average. For galaxies where these effects changed the type from a spiral classification to S0 or SB0, we have used the index $T = -2$.

Table 6 summarizes the mean values by stage and family from the near-IR classifications. As noted by Eskridge et al. (2000), near-IR classifications from the OSU sample show twice as many strongly barred (SB) types as in the optical. However, Table 6 shows that the Eskridge et al. SAB and SB classifications have slightly lower $\langle Q_g \rangle$ than the corresponding RC3 families. RC3 SB galaxies in our sample have $\langle Q_g \rangle = 0.331 \pm 0.019$ (mean error), while Eskridge et al. SB galaxies in our sample have $\langle Q_g \rangle = 0.290 \pm 0.015$. The likely reason for this difference is that near-IR images not only make weak bars more evident but also make stronger bars more obvious. Thus, near-IR imaging does not necessarily change the rankings of bars much. There is no new category for a B -band

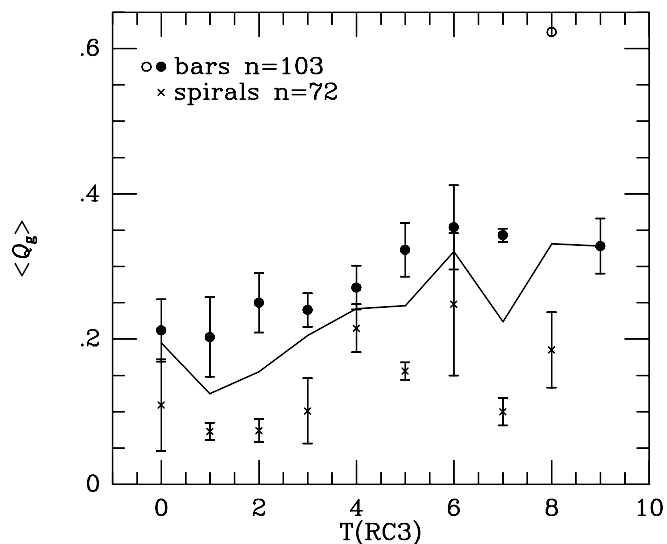


FIG. 15.—Plot of $\langle Q_g \rangle$ vs. RC3 type index separated according to whether the radius of the Q_T maximum occurs in the bar-dominated region (filled circles) or the spiral-dominated region (crosses). The open circle is based on only one galaxy. The plot demonstrates that both spirals and bars have relatively weaker torques in early-type spirals as compared to late-type spirals. The solid curve shows the means from Table 5.

SB spiral to be placed into even though its bar looks stronger in the near-IR. However, a B -band SAB spiral can be placed into the SB category if it looks stronger in the near-IR. Since the real rankings are not changed much, the mean $\langle Q_g \rangle$ for the near-IR families is decreased because of inclusion of weaker bars.

Figure 17 shows that when $\langle Q_g \rangle$ is plotted against the numerically coded near-IR stages, a strong trend with type is seen that extends into the near-IR S0 class. The trend is smoother than that found using RC3 types but has about the same amplitude from S0/a to Sm. The improved correlation is probably not unexpected since the appearance of the spiral arms helped to determine the near-IR type and the strength of the arms can impact Q_g . For example, the spiral arms in some of the OSU galaxies are virtually invisible in the near-IR, leading to a classification of S0. However, the implication

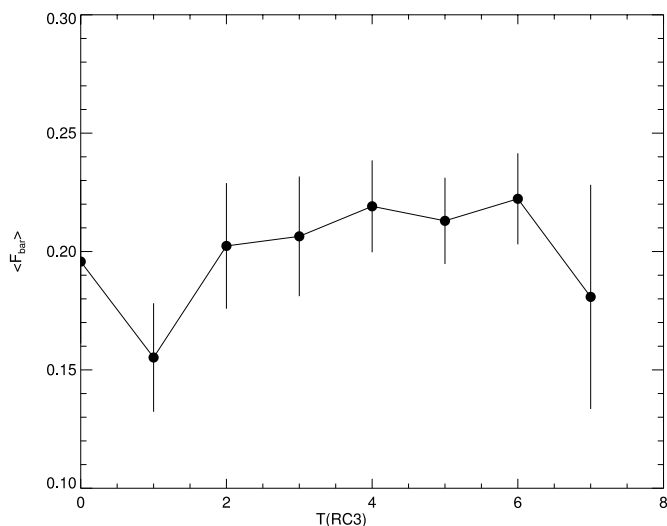


FIG. 16.—Average bar strength parameter f_{bar} from Whyte et al. (2002) vs. RC3 type index.

TABLE 6
MEAN MAXIMUM RELATIVE TORQUE BY NEAR-INFRARED REVISED HUBBLE CLASSIFICATION

Stage or Family	$\langle Q_g \rangle$	σ	Mean Error	n
S0	0.103	0.070	0.022	10
S0/a	0.147	0.095	0.024	15
Sa	0.191	0.124	0.025	24
Sab	0.238	0.121	0.029	18
Sb	0.220	0.143	0.027	28
Sbc	0.269	0.168	0.037	20
Sc	0.284	0.152	0.044	12
Scd	0.320	0.200	0.067	9
Sd	0.361	0.177	0.056	10
Sdm	0.318	0.111	0.045	6
Sm	0.297	0.063	0.032	4
S0–Sb	0.159	0.110	0.016	49
Sbc–Sm	0.265	0.158	0.016	97
S	0.116	0.082	0.014	32
SAB	0.174	0.112	0.022	26
SB	0.290	0.147	0.015	98

NOTE.—Classifications are from col. (5) of Table 1 of Eskridge et al. 2002.

once again is that maximum relative torques are weaker in early-type disk galaxies than in late-type disk galaxies.

11. CONCLUSIONS

We have derived an accurate distribution of maximum relative gravitational torques in a sample of 180 OSUBGS and 2MASS galaxies. The sample is representative of bright galaxies but is biased against late-type, low-luminosity barred spirals. It is not biased against nonbarred galaxies. The distribution is more accurate than previous studies because of the refinement of the gravitational torque method. We have used two-dimensional bulge/disk/bar decomposition to eliminate the impact of bulge deprojection stretch on the calculated torques and to derive reliable radial scale lengths that can be scaled to vertical scale heights using the type dependence of h_R/h_z derived by de Grijs (1998). We have also used orientation parameters based on isophotal ellipse fits to the blue-light images in the OSUBGS, which are an

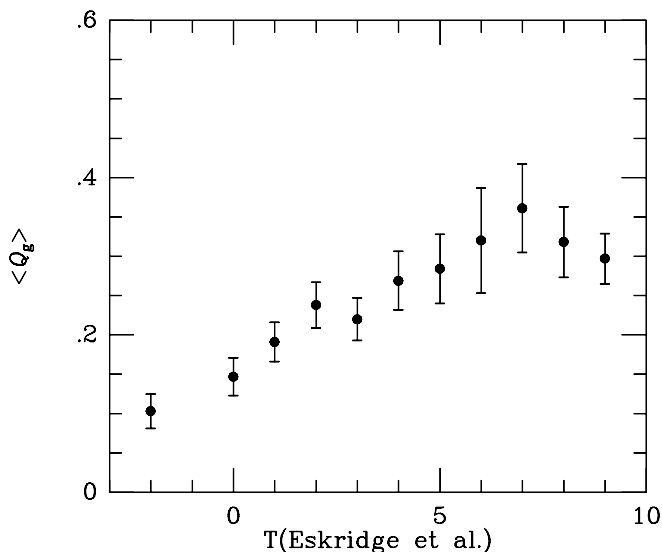


FIG. 17.—Mean maximum relative torque vs. the near-infrared type from Eskridge et al. (2002) for 146 OSUBGS galaxies.

improvement over previously published values for many of the galaxies. With these refinements, we find a higher frequency of low maximum relative torque galaxies compared to Block et al. (2002). The implications for the amount of accreted matter advocated by Block et al. (2002) remain to be evaluated, but we expect that the revised distribution will favor less accretion once the models account for the same refinements the observations have accounted for. This will be addressed in a future paper.

We have discussed in detail the uncertainties and biases in our distribution of gravitational torques. Because the sample emphasizes high-luminosity systems, corrections for dark matter appear to be small. In the future, further improvements could be made by obtaining two-dimensional velocity fields of the galaxies in question. This would facilitate the derivation of kinematic orientation parameters and improved deprojections.

We find a significant dependence of the mean maximum gravitational torque on revised Hubble type. The effect persists even when the sample is divided into bar-dominated and spiral-dominated subsamples and when near-infrared types from Eskridge et al. (2002) are used in place of RC3 types. Both bars and spirals tend to have weaker average relative torques in early-type spirals compared to late-type spirals. The likely cause of this is torque dilution due to the stronger bulges in early-type spirals. Dark matter has only a marginal impact on this effect.

We thank the referee, F. Combes, for valuable comments on our paper and for sending a file with her estimates of Q_g for the OSU sample. We also thank L. Whyte for sending her table of f_{bar} values. R. B. acknowledges the support of NSF grant AST 02-05143 to the University of Alabama. E. L. and H. S. acknowledge the support of the Academy of Finland, and E. L. also acknowledges support from the Magnus Ehrnrooth Foundation. Funding for the OSU Bright Galaxy Survey was provided by grants from the National Science Foundation (AST 92-17716 and AST 96-17006), with additional funding from the Ohio State University. This

publication also utilized images from the Two Micron All Sky Survey, which is a joint project of the University of Massachusetts and the Infrared Processing and Analysis Center of the California Institute of Technology, funded by the National Aeronautics and Space Administration and the

National Science Foundation. This research has also made use of the NASA/IPAC Extragalactic Database (NED), which is operated by the Jet Propulsion Laboratory, California Institute of Technology, under contract with the National Aeronautics and Space Administration.

REFERENCES

- Abraham, R. G., & Merrifield, M. R. 2000, *AJ*, 120, 2835
 Bell, E. F., & de Jong, R. S. 2001, *ApJ*, 550, 212
 Block, D. L., Bournaud, F., Combes, F., Puerari, I., & Buta, R. 2002, *A&A*, 394, L35
 Block, D. L., Puerari, I., Knapen, J. H., Elmegreen, B. G., Buta, R., Stedman, S., & Elmegreen, D. M. 2001, *A&A*, 375, 761
 Bournaud, F., & Combes, F. 2002, *A&A*, 392, 83
 Buta, R., & Block, D. L. 2001, *ApJ*, 550, 243
 Buta, R., Block, D. L., & Knapen, J. H. 2003, *AJ*, 126, 1148
 Buta, R., & Combes, F. 1996, *Fundam. Cosmic Phys.*, 17, 95
 Combes, F., & Sanders, R. H. 1981, *A&A*, 96, 164
 Das, M., Teuben, P. J., Vogel, S. N., Regan, M. W., Sheth, K., Harris, A. I., & Jefferys, W. H. 2003, *ApJ*, 582, 190
 de Grijs, R. 1998, *MNRAS*, 299, 595
 de Vaucouleurs, G. 1959, *Handbuch der Physik*, 53, 275
 de Vaucouleurs, G., et al. 1991, *Third Reference Catalog of Bright Galaxies* (New York: Springer) (RC3)
 Elmegreen, B. G., & Elmegreen, D. M. 1985, *ApJ*, 288, 438
 Eskridge, P., et al. 2000, *AJ*, 119, 536
 ———. 2002, *ApJS*, 143, 73
 Freeman, K. C. 1970, *ApJ*, 160, 811 (erratum 161, 802)
 ———. 1992, in *Physics of Nearby Galaxies: Nature or Nurture?* ed. T. X. Thuan, C. Balkowski, & J. Trân Thanh Vân (Gif-sur-Yvette: Editions Frontières), 201
 Gilmore, G., & Reid, N. 1983, *MNRAS*, 202, 1025
 Hohl, F. 1971, *ApJ*, 168, 343
 Kormendy, J. 1993, in *IAU Symp. 153, Galactic Bulges*, ed. H. DeJonghe & H. J. Habing (Dordrecht: Kluwer), 209
 Kormendy, J., & Norman, C. 1979, *ApJ*, 233, 539
 Kranz, T., Slyz, A., & Rix, H.-W. 2003, *ApJ*, 586, 143
 Laurikainen, E., & Salo, H. 2002, *MNRAS*, 337, 1118
 Laurikainen, E., Salo, H., Buta, R., & Vasylyev, S. 2003, in preparation
 Laurikainen, E., Salo, H., & Rautiainen, P. 2002, *MNRAS*, 331, 880
 Martin, P., & Roy, J.-R. 1994, *ApJ*, 424, 599
 McCall, M. L. 1986, *PASP*, 98, 992
 Miller, R. H., Prendergast, K. H., & Quirk, W. J. 1970, *ApJ*, 161, 903
 Miwa, T., & Noguchi, M. 1998, *ApJ*, 499, 149
 Mollenhöff, C., & Heidt, J. 2001, *A&A*, 368, 16
 Noguchi, M. 1996, *ApJ*, 469, 605
 Norman, C. A., Sellwood, J. A., & Hasan, H. 1996, *ApJ*, 462, 114
 Persic, M., Salucci, P., & Stel, F. 1996, *MNRAS*, 281, 27 (erratum 283, 1102) (PSS)
 Quillen, A. C., Frogel, J. A., & González, R. A. 1994, *ApJ*, 437, 162 (QFG)
 Roberts, W. W., Roberts, M. S., & Shu, F. H. 1975, *ApJ*, 196, 381
 Salo, H., Laurikainen, E., & Buta, R. 2003, in preparation
 Sandage, A., & Bedke, J. 1994, *Carnegie Atlas of Galaxies* (Publ. 638; Washington, DC: Carnegie Inst.)
 Sanders, R. H., & Tubbs, A. D. 1980, *ApJ*, 235, 803
 Schwarz, M. P. 1981, *ApJ*, 247, 77
 Sellwood, J. A. 2000, in *ASP Conf. Ser. 197, Dynamics of Galaxies: From the Early Universe to the Present*, ed. F. Combes, G. A. Mamon, & V. Charmandaris (San Francisco: ASP), 3
 Sellwood, J. A., & Moore, E. M. 1999, *ApJ*, 510, 125
 Sellwood, J. A., & Wilkinson, A. 1993, *Rep. Prog. Phys.*, 56, 173
 Sérsic, J. L. 1968, *Atlas de Galaxias Australes* (Cordoba: Obs. Astron. Univ. Nac. Cordoba)
 Skrutskie, M. F., et al. 1997, in *The Impact of Large Scale Near-IR Surveys*, ed. F. Grazon et al. (Dordrecht: Kluwer), 25
 Tully, R. B. 1988, *Nearby Galaxies Catalogue* (Cambridge: Cambridge Univ. Press)
 Whyte, L., Abraham, R. G., Merrifield, M. R., Eskridge, P. B., Frogel, J. A., & Pogge, R. W. 2002, *MNRAS*, 336, 1281